



# Surfactant-assisted hydrothermal crystallization of nanostructured lithium metasilicate ( $\text{Li}_2\text{SiO}_3$ ) hollow spheres: II—Textural analysis and $\text{CO}_2$ – $\text{H}_2\text{O}$ sorption evaluation

José Ortiz-Landeros<sup>b</sup>, Carlos Gómez-Yáñez<sup>b</sup>, Heriberto Pfeiffer<sup>a,\*</sup>

<sup>a</sup> Instituto de Investigaciones en Materiales, Universidad Nacional Autónoma de México, Circuito exterior s/n, Ciudad Universitaria, Del. Coyoacán, CP 04510 México DF, Mexico

<sup>b</sup> Departamento de Ingeniería en Metalurgia y Materiales, Escuela Superior de Ingeniería Química e Industrias Extractivas, IPN, Av. Instituto Politécnico Nacional s/n, CP 07738 México DF, Mexico

## ARTICLE INFO

### Article history:

Received 4 December 2010

Received in revised form

2 June 2011

Accepted 23 June 2011

Available online 1 July 2011

### Keywords:

Lithium metasilicate

Hydrothermal crystallization

Textural analysis

$\text{H}_2\text{O}$  adsorption

$\text{CO}_2$  absorption

## ABSTRACT

In a previous work, the synthesis and structural-microstructural characterization of different nano-crystalline lithium metasilicate ( $\text{Li}_2\text{SiO}_3$ ) samples were performed. Then, in this work, initially, a textural analysis was performed over the same samples.  $\text{Li}_2\text{SiO}_3$  samples prepared with a non-ionic surfactant (TRITON X-114) presented the best textural properties. Therefore, this sample was selected to evaluate its water vapor ( $\text{H}_2\text{O}$ ) and carbon dioxide ( $\text{CO}_2$ ) sorption properties. Sorption experiments were performed at low temperatures (30–80 °C) in presence of water vapor using  $\text{N}_2$  or  $\text{CO}_2$  as carrier gases. Results clearly evidenced that  $\text{CO}_2$  sorption on these materials is highly improved by  $\text{H}_2\text{O}$  vapor, and of course, textural properties enhanced the  $\text{H}_2\text{O}$ – $\text{CO}_2$  sorption efficiency, in comparison with the solid-state reference sample.

© 2011 Elsevier Inc. All rights reserved.

## 1. Introduction

Lithium ceramics have been reported for several potential applications including the fabrication of ceramic breeders, ionic conductors, gas sensors and solid sorbents for  $\text{CO}_2$  capture [1–13]. Such is the case of lithium metasilicate ( $\text{Li}_2\text{SiO}_3$ ), which has been reported as promising tritium breeder material into the fusion reactors [14,15], as an ionic conductor [16,17] and as candidate for luminescent devices [18,19].

Usually,  $\text{Li}_2\text{SiO}_3$  is synthesized by solid-state reaction, but also a few chemical routes have been studied [20–22]. These studies have shown the feasibility to fabricate  $\text{Li}_2\text{SiO}_3$  for novel potential applications. Among these chemical routes, Khomane et al. [21] reported the synthesis of  $\text{Li}_2\text{SiO}_3$  nanoparticles by coupling sol–gel method in reverse microemulsion. The obtained powders showed the ability to absorb  $\text{CO}_2$  under certain conditions, where it was assumed that the synthesis route increased the reactivity of  $\text{Li}_2\text{SiO}_3$  as a result of its small particle size and then, its high surface area.

In this context, different factors can limit the  $\text{CO}_2$  capture process on lithium ceramics; for example, particle size and lithium diffusion [13]. Hence, several studies have been performed in order to elucidate

the absorption mechanism as well as on possible microstructural, structural and/or chemical modifications of these alkaline ceramics sorbents, seeking to enhance efficiency and  $\text{CO}_2$  absorption rates [11–13].

The chemical route used in this work was chosen to obtain particulate materials with microstructural and textural characteristics that could promote their performance for novel applications such as  $\text{CO}_2$  sorption. In fact, in a previous work [23], we have described in detail the systematic hydrothermal synthesis and characterization of these nanostructured  $\text{Li}_2\text{SiO}_3$  samples. Therefore, in the present work it is discussed, not only the effect of synthesis route on the characteristics of synthesized  $\text{Li}_2\text{SiO}_3$  powders, but also their capability to absorb  $\text{CO}_2$  at low temperature, giving a special emphasis to textural characteristics of solid sorbents and the effect of water vapor addition during  $\text{CO}_2$  capture process.

## 2. Experimental procedure

$\text{Li}_2\text{SiO}_3$  samples were prepared by hydrothermal synthesis using three different surfactants (CTAB, TRITON X-114 and SDBS) at 100, 125 and 175 °C [23]. The obtained powders were washed, and calcined at 400 °C. Samples were labeled by a number, which correspond to hydrothermal synthesis temperature, followed by an abbreviation, indicating the surfactant used and the letter C indicating the calcination process. Samples prepared without

\* Corresponding author. Fax: +52 55 56161371.

E-mail address: [pfeiffer@iim.unam.mx](mailto:pfeiffer@iim.unam.mx) (H. Pfeiffer).

surfactant were simply labeled by a number indicating the temperature used during synthesis. More details about the hydrothermal synthesis of the powders, as well as the corresponding structural and microstructural characteristics, had been already published [23]. Summarizing, it could be mentioned that  $\text{Li}_2\text{SiO}_3$  powders were composed of uniform micrometric particles with a hollow sphere morphology and nanostructured walls. Finally, different thermal analyses showed that  $\text{Li}_2\text{SiO}_3$  samples preserved their structure and microstructure even after different thermal treatments.

Textural properties of  $\text{Li}_2\text{SiO}_3$  samples were evaluated by  $\text{N}_2$  physisorption isotherms, which were measured using a BEL-Japan apparatus model Minisorp-II. Different mathematical models, such as BET and  $\alpha_s$  methods, were utilized to analyze the isotherms.

Once all samples were characterized, some of these samples were subjected to different dynamic water vapor and  $\text{CO}_2$  sorption tests. Experiments were carried out in a temperature-controlled thermobalance TA Instruments model Q5000SA, where experimental variables were temperature, relative humidity (RH) and the carrier gas ( $\text{CO}_2$  or  $\text{N}_2$ , both provided by Praxair). First, water vapor sorption/desorption isotherms were generated at 30, 50 and 70 °C, varying the relative humidity from 0% to 85% to 0% under a  $\text{N}_2$  flux. Additionally, in order to evaluate the capability of  $\text{Li}_2\text{SiO}_3$  to absorb  $\text{CO}_2$  at low temperature, different sorption curves were obtained maintaining the above experimental conditions, but in this case under a  $\text{CO}_2$  flux. In order to identify the reaction products, humidity test products were characterized by thermogravimetry (TG) and infrared (FTIR) spectroscopy after sorption experiments. For TG analyses, experiments were performed under air atmosphere with a heating rate of 3 °C/min using a thermobalance TA Instruments model Q500HR. For FTIR analysis, samples were analyzed by diffuse reflectance using a FTIR Spectrometer NICOLET 6700 FT-IR.

### 3. Results and discussion

As it has been already shown in a previous paper [23], all the hydrothermal synthesis performed with or without surfactant produced nanostructured  $\text{Li}_2\text{SiO}_3$  hollow spheres, independent of the temperature. Fig. 1 shows the adsorption–desorption isotherms of the same hydrothermal samples prepared at 100 °C and reported previously [23], using different surfactants and the one prepared by solid-state reaction. According to the IUPAC classification [24,25], all samples present isotherms type II, which are attributed not only to monolayer–multilayer adsorption on an open external surface of non-porous or macroporous adsorbents, but also, to a limited extend, microporous powder. On the other hand, applying the BET method, C values were obtained in the 120–190 range, which suggest a relatively strong adsorbent–adsorbate interaction, but since the point B is not as sharper as could be expected (Fig. 1), then high C values were attributed to the presence of certain heterogeneous adsorption.

In this case, the presence of certain microporosity can be ruled out because of both, the small gas volume that was adsorbed at low partial pressure values and the obtained C values ( $< 200$ ) [24]. Hysteresis loops are type H3, and non-stepwise is observed, that is usually interpreted as a result of presence of slit-like pores. In addition, it is noticeable that volume adsorbed decreases considerably for sample prepared by solid state reaction, which corroborates the formation of more dense particles due to a sintering process. Textural characteristics of the different samples after thermal treatment at 400 °C are presented in Table 1. It is evident that all hydrothermally samples exposed higher surfaces area values than the sample obtained by solid-state reaction. The highest surface area values correspond to samples, which were prepared using surfactant. Besides, the effect of hydrothermal

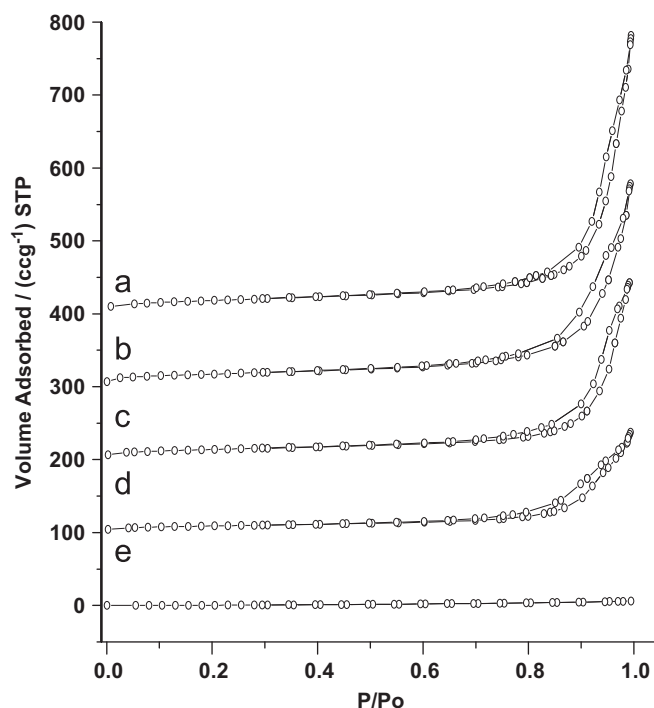


Fig. 1.  $\text{N}_2$  physisorption isotherms of samples prepared with different surfactants: (a) 100TRITC, (b) 100SDBSC, (c) 100CTABC, (d) 100C and (e) solid-state reaction.

Table 1  
Textural properties of different samples.

Sample	Textural properties		
	$\alpha_s$ , BET ( $\text{m}^2 \text{g}^{-1}$ )	Total pore volume ( $\text{cm}^3 \text{g}^{-1}$ )	Mean pore diameter (nm)
Solid-state	0.47	–	–
100C	31.9	0.199	26.02
125C	22.3	0.038	6.9
175C	13.4	0.02	4.9
100TRITC	66.9	0.529	33.7
125TRITC	56.9	0.501	35.9
175TRITC	24.2	0.263	43.9

temperature on textural properties of samples synthesized is also observed. It can be noticed a decrease on both, surface area and pore volume, at higher reaction temperatures, as it could be expected due to crystal growth.

In spite of the high C values suggest the validity of the standard BET procedure to calculate the surface area values, the  $\alpha_s$ -method was also applied, in order to validate BET results. Fig. 2 shows the  $\alpha_s$  plot of sample 100TRITC. The used standard isotherm was silica; this reference curve data was available at the equipment software data base. Specific surface area value was estimated as  $68.2 \text{ m}^2 \text{g}^{-1}$ . This value agrees with that one calculated by BET method (see Table 1), which validates the obtained areas.

In general, all samples presented pore sizes in the mesoporosity range (Table 1). However, it is important to mention that based on the previous results, it would be inferred that porous structure is composed of interparticle voids. Besides, since the obtained hysteresis loops are type H3; then, the estimated pore sizes are showed only for comparative purposes. The different obtained pore sizes are attributed to surfactant addition. Bigger pore sizes were obtained when TRITON-X114 surfactant was used. These textural characteristics are important for applications such as absorption where the reactivity plays an important role. Other advantages could be based on the fact that fast mass

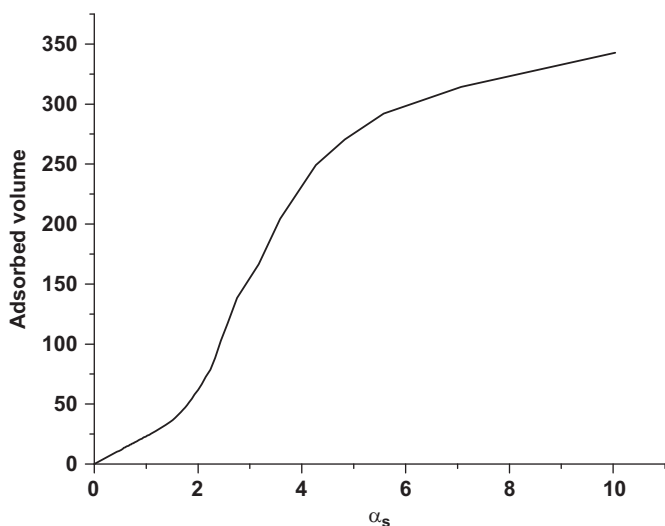


Fig. 2.  $\alpha_s$ -Plot corresponding to sample 100TRITC.

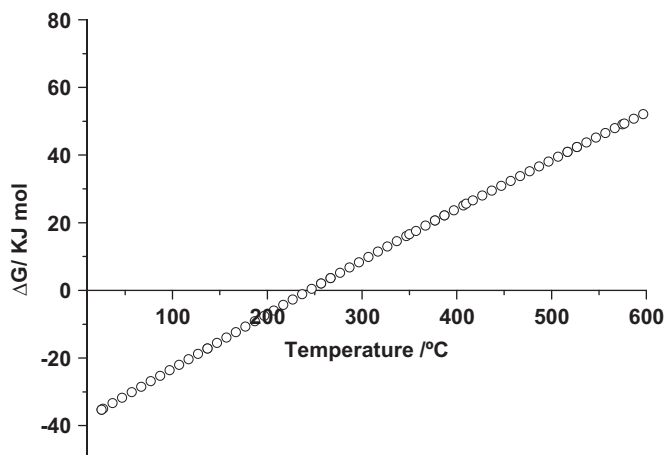


Fig. 3. Gibbs free energy change as a function of the temperature for reaction (1).

transference inside the agglomerate-particles could be improved by this kind of textures [26].

To further analyze and test these materials,  $\text{CO}_2$  sorption in presence of water vapor was studied. Based on theoretical thermodynamic data calculated by FACTSage software [27], a reversible reaction between  $\text{Li}_2\text{SiO}_3$  and  $\text{CO}_2$  can take place at temperatures lower than  $250^\circ\text{C}$  (Fig. 3).



In fact, Khomane et al. [21] reported that  $\text{CO}_2$  capture on  $\text{Li}_2\text{SiO}_3$  occurs in spite of its low reactivity and kinetic factors. Of course, reaction was carried out at temperature up to  $600^\circ\text{C}$  and under specific conditions of pressure and small particle size with relatively high surface areas values ( $7\text{ m}^2\text{ g}^{-1}$ ). On the other hand, some researchers have reported water vapor addition effects on  $\text{CO}_2$  capture of lithium ceramics. They observed that water addition enhances kinetic properties even at low temperatures [28–31]. So, with these antecedents, and taking into consideration the novel textural properties observed in the synthesized materials, studies of low temperature  $\text{CO}_2$  absorption on  $\text{Li}_2\text{SiO}_3$  in presence of water were carried out. The selected samples were 100C and 100TRITC, but also sample prepared by solid state reaction was tested as a reference.

First, selected samples were exposed to water vapor at 30, 50 and  $70^\circ\text{C}$ , using  $\text{N}_2$  as carrier gas. These experiments were performed to

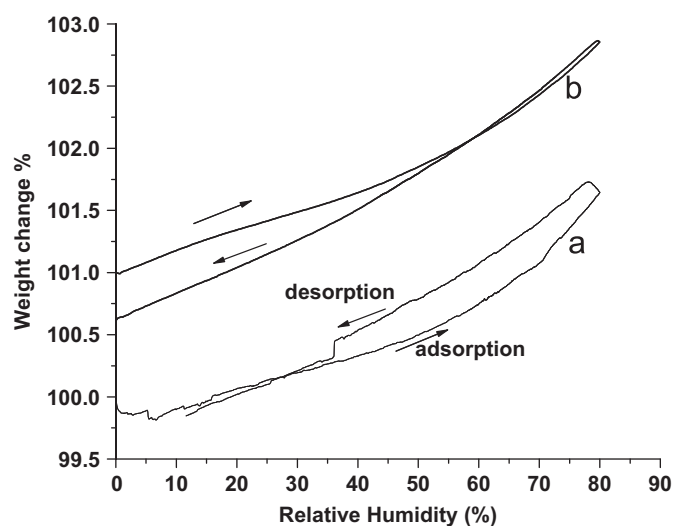


Fig. 4. Isotherms of water adsorption/desorption in the sample 100TRITC at different relative humidity (RH) conditions, under  $\text{N}_2$  flux and temperature of (a)  $30^\circ\text{C}$  and (b)  $70^\circ\text{C}$ .

seek for any possible reaction between lithium metasilicate and water vapor. Fig. 4 shows water vapor adsorption/desorption isotherms, which were generated for sample 100TRITC at temperatures of 30 and  $70^\circ\text{C}$ . These water vapor adsorption isotherms belong to type III, according to the IUPAC, which indicates a relative weak adsorbate–adsorbent interaction. In the adsorption stage, weight increments, of about 1.82% and 1.86 wt%, were registered for samples treated at 30 and  $70^\circ\text{C}$ , respectively (Fig. 4). After that, during desorption stage, sorption hysteresis is observed. However, hysteresis loops tend to close indicating that a reversible process took place, and weight increments were due to physisorbed water.

When samples were treated under a mixture of  $\text{CO}_2$  and water vapor, a totally different sorption behavior was observed. Fig. 5 shows the water vapor isotherms of these samples synthesized at  $100^\circ\text{C}$  without surfactant addition (Fig. 5a) and using TRITON X-114 (Fig. 5b). In both cases, during sorption stage, important increments in the weight change were registered as a function of temperature. Even during desorption, weight increments continued and hysteresis loops did not close. In fact, at the end of sorption–desorption cycles important final weight increments were registered, suggesting a chemical process. It is important to mention that, in spite of thermodynamic data indicate that reaction between  $\text{Li}_2\text{SiO}_3$  and  $\text{CO}_2$  could occur spontaneously at low temperatures ( $\Delta G < 0$  at  $T < 250^\circ\text{C}$ ),  $\text{CO}_2$  is not absorbed in absence of water vapor. This fact must be due to kinetic factors associated to surface area and textural properties, as it is shown below when solid-state sample is compared.

Additionally, it is noticeable that not only water vapor but also surface area has a crucial effect on  $\text{Li}_2\text{SiO}_3$  reaction with  $\text{CO}_2$ . In Fig. 6, the sorption isotherms of solid-state, 100C and 100TRITC samples are shown. While solid-state sample does not absorb  $\text{CO}_2$ , samples with higher surface areas absorbed up to 37.5 wt% under the same experimental conditions (Table 2). Based on reaction (1), theoretically, lithium metasilicate could absorb a maximum of  $\text{CO}_2$  equal to 48.9 wt%. The maximum weight increment registered after sorption corresponded to 37.5 wt% for the 100TRITC sample thermally treated at  $70^\circ\text{C}$ . However, it is important to have in mind that the presence of water vapor could promote the formation of hydrated and/or hydroxylated products. Then, in order to analyze the reaction products, they were characterized by FTIR and TGA.

Fig. 7 shows FTIR spectra of the 100TRITC sample before and after the humidity treatments at 30 and  $70^\circ\text{C}$ , using  $\text{N}_2$  as carrier gas, respectively. All these spectra do not present any significant

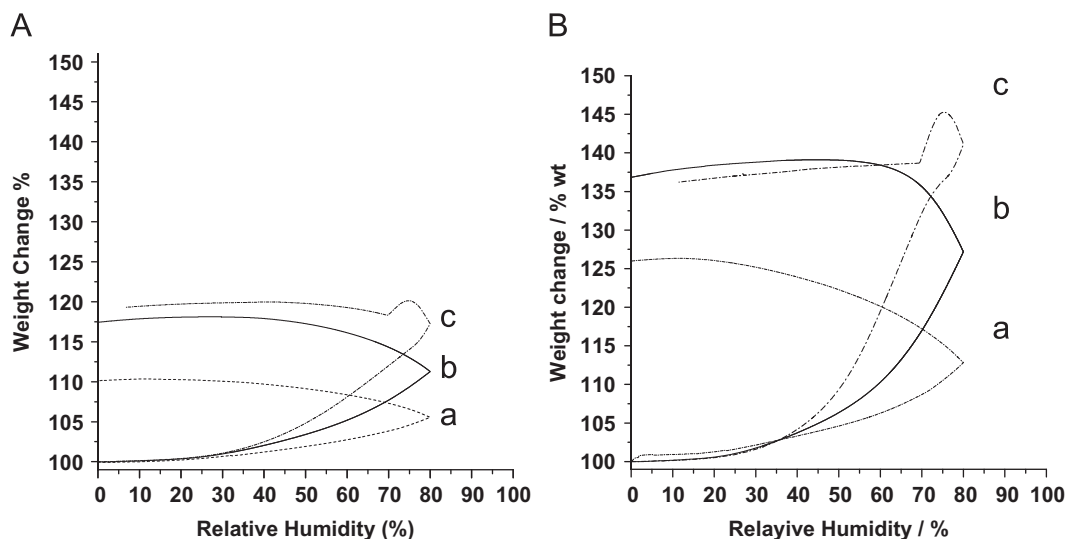


**Fig. 5.** CO<sub>2</sub> and water vapor sorption on Li<sub>2</sub>SiO<sub>3</sub> particles in a dynamic process at different relative humid (RH) conditions (0–85–0%RH), and temperatures: Panel (A) corresponds to the sample 100C at (a) 30 °C, (b) 50 °C and (c) 70 °C and panel (B) corresponds to the sample 100TRITC at (a) 30 °C, (b) 50 °C and (c) 70 °C.

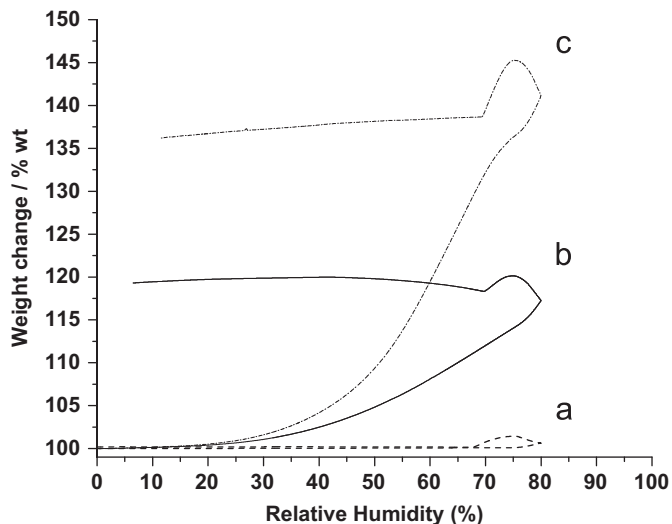


**Fig. 6.** CO<sub>2</sub> and water vapor sorption on Li<sub>2</sub>SiO<sub>3</sub> particles in a dynamic process at different relative humid (RH) conditions (0–85–0%RH), and temperature of 70 °C. Isotherms correspond to different samples: (a) solid-state reaction, (b) 100C, (c) 100TRITC.

**Table 2**

Weight changes during CO<sub>2</sub>–H<sub>2</sub>O sorption for the different samples.

Temp. (°C)	Weight increments observed during sorption processes (wt%)					
	Solid-state		100C		100TRITC	
	Sorption	After desorp.	Sorption	After desorp.	Sorption	After desorp.
30	0.19	0.20	5.55	10.2	12.87	26.4
50	0.09	0.10	11.29	17.6	27.50	38.3
70	0.63	0.20	17.28	19.5	41.42	37.5

variation among them. Vibration bands at 411 and 491 cm<sup>-1</sup> are due to vibrations of the terminal Si–O and Li–O bonds [20], respectively. The bands located at 615, 736, 981 and 1050 cm<sup>-1</sup> correspond to Si–O–Si bonds. The bands at 857 and 938 cm<sup>-1</sup> were assigned to O–Si–O<sup>-</sup> and O–Si–O bonds vibration, respectively. Besides the band at 1436 cm<sup>-1</sup> was attributed to presence

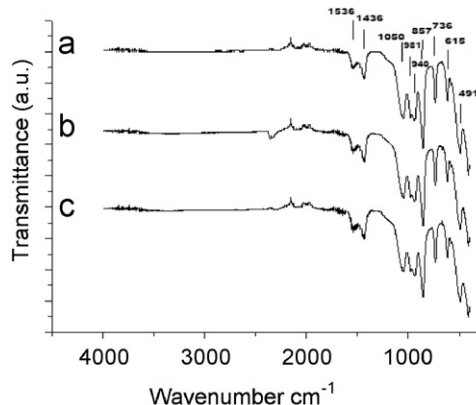


**Fig. 7.** Infrared spectra of the Li<sub>2</sub>SiO<sub>3</sub> samples recorded after humidity treatment under N<sub>2</sub> flux: (a) sample 100TRITC without any treatment, (b) sample treated at 30 °C, and (c) sample treated at 70 °C.

of Li<sub>2</sub>CO<sub>3</sub> on lithium metasilicate particle surface. These results suggest that lithium metasilicate seems not to react with water vapor under the studied conditions.

On the other hand, FTIR spectra of samples treated under a water vapor and CO<sub>2</sub> flux (Fig. 8), corroborate the CO<sub>2</sub> absorption on lithium metasilicate by the formation of Li<sub>2</sub>CO<sub>3</sub> according to reaction (1). In this case, the band located at 491 cm<sup>-1</sup> disappears when the treatment temperature increased. Since this band is attributed to terminal bonds surface reaction occurs on these surface active sites, as expected. There is another group of bands, which decrease in intensity after reaction; this group includes the bands located at 615, 736 and 981 cm<sup>-1</sup>. All these signals correspond to Si–O–Si vibration bonds on silicate. On the contrary, it is clear that 1436 and 1050 cm<sup>-1</sup> bands increased in intensity. Then, if it is kept in mind that CO<sub>2</sub> absorption products are Li<sub>2</sub>CO<sub>3</sub> and, SiO<sub>2</sub> then it can be assumed that these last two bands correspond to lithium carbonate and Si–O–Si (asymmetric stretch) on formed silica, respectively. This claim is also supported by the fact that the presence of small bands at 470 and 798 cm<sup>-1</sup> are a consequence of Si–O–Si bend and symmetric stretch of silica [32,33].

Finally, a thermal analysis of reaction products was carried out. The TG curves exhibit important weight-losses (Fig. 9). Initially, between room temperature and 150 °C, samples lost adsorbed water from hydration. However, it was not higher than

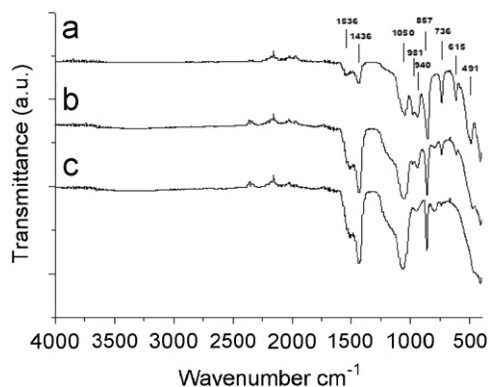


**Fig. 8.** Infrared spectra of the  $\text{Li}_2\text{SiO}_3$  samples recorded after humidity treatment under  $\text{CO}_2$  flux: (a) 100TRITC sample without any treatment, (b) 100TRITC sample treated at 30 °C, and (c) 100TRITC sample at 70 °C.

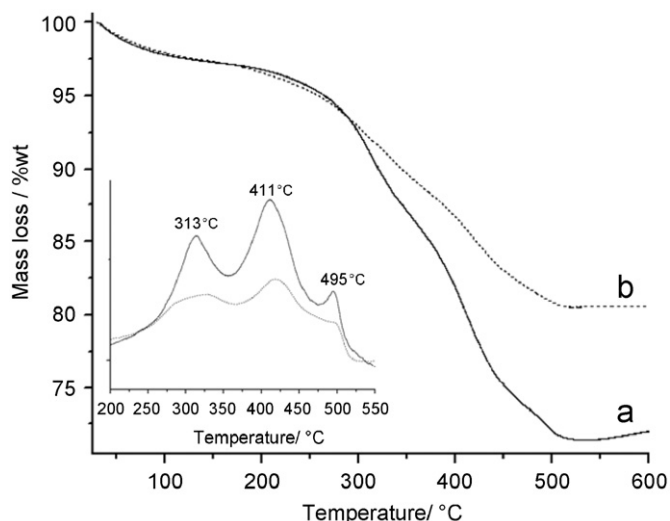


**Fig. 9.** TGA curves for different  $\text{Li}_2\text{SiO}_3$  samples after humidity treatment under  $\text{CO}_2$  flux: (a) 100TRITC sample without any treatment and (b) 100TRITC sample treated at 70 °C. The inset shows the derivative curve of thermogravimetric data.

3 wt%. The second weight loss began at about 313 °C, and it is more likely due to decomposition of carbonates [31].

Once  $\text{CO}_2$  absorption on  $\text{Li}_2\text{SiO}_3$  was corroborated, it is necessary to understand how the capture process take place. Although some authors have suggested that water exposure can inhibit  $\text{CO}_2$  absorption on some lithium ceramics [11], in general, there is an agreement that the presence of water vapor promotes  $\text{CO}_2$  absorption on alkaline ceramics as well as in some other ceramic compounds such as hydrotalcites [34]. In fact, different mechanisms of  $\text{CO}_2$  capture in presence of water vapor have been proposed [28–31]. Essaki et al. [29] found that humidity increases  $\text{CO}_2$  absorption on lithium orthosilicate  $\text{Li}_4\text{SiO}_4$  at room temperature. Authors proposed a capture mechanism where acid-base reactions with hydrolysis of  $\text{CO}_2$  and  $\text{Li}_2\text{O}$  are involved. They also suggested that carbonate layer formed on the ceramic surface during absorption, might be dissolved in water thus, in this way, absorption is promoted. Siasinus et al. [30] studied the carbonation of Tobermorite powders stressing the effect of both textural properties of the sorbent and the presence of water vapor during the process. In this case (similarly to Essaki et al. conclusions), authors suggested an intermediate hydrolysis reaction but additionally they consider the formation of more reactive species into the Tobermorite structure as a result of its textural properties. Ochoa-Fernandez et al. [28] studied the effect of water vapor addition on the  $\text{CO}_2$  capture at elevated temperatures by lithium zirconates ( $\text{Li}_2\text{ZrO}_3$ , K-doped

$\text{Li}_2\text{ZrO}_3$  and  $\text{Na}_2\text{ZrO}_3$ ) and  $\text{Li}_4\text{SiO}_4$  ceramics. Ceramics presented improvements on the  $\text{CO}_2$  absorption and desorption processes due to the presence of water vapor. They concluded that water vapor promotes alkaline ions mobility and therefore the reaction rate. In a more recent work Martinez-dlCruz and Pfeiffer [31] reported the effect of water sorption on  $\text{Li}_2\text{ZrO}_3$  and K-doped  $\text{Li}_2\text{ZrO}_3$  during their carbonation at low temperatures. They found that  $\text{CO}_2$  absorption on these ceramic is proportional to its reactivity with water vapor. They concluded that during  $\text{CO}_2$  capture on alkaline ceramics (specially on lithium zirconate which has the capacity to react with water) the formation of intermediate species like M–OH is involved, since these species are more prone to react with  $\text{CO}_2$  than the adsorbent itself, leading to a general increase in the kinetic of capture. In fact,  $\text{Li}_4\text{SiO}_4$  chemisorbs water vapor at a similar thermal conditions than the present work, forming Si–OH and Li–OH species [35].

Based on the above results, more than one mechanism might be taking place in this system. However, thermodynamic data show that the following reaction (2) do not occur spontaneously:



In fact, this claim is supported by the experimental results since the reaction was not observed (Figs. 6a and 7). Then, in the  $\text{Li}_2\text{SiO}_3\text{--CO}_2\text{--H}_2\text{O}$  system the formation of intermediate species must be promoted by the porous microstructures, large surface areas and aqueous environment. All these factors must induce the beginning of  $\text{CO}_2$  reaction in active sites such as terminal bonds and, perhaps, enriched lithium zones on the solid.

#### 4. Conclusions

Pure and nanocrystalline  $\text{Li}_2\text{SiO}_3$  samples with high surface area values (as high as  $66.9 \text{ m}^2 \text{ g}^{-1}$ ) were previously synthesized by hydrothermal method.  $\text{Li}_2\text{SiO}_3$  samples prepared with TRITON X-114, a surfactant, presented the best textural properties. In general, surfactant addition and hydrothermal temperatures played crucial roles to control morphology and microstructure, resulting in the formation of spherical hollow aggregates which present novel microstructural and textural characteristics. Despite, the water vapor does not seem to modify substantially the  $\text{Li}_2\text{SiO}_3$  surface, the combination of  $\text{CO}_2$  and water vapor enhances importantly the  $\text{CO}_2$  capture on  $\text{Li}_2\text{SiO}_3$  at low temperatures.  $\text{CO}_2$  capture occurred chemically and this reaction was enhanced by the porous microstructure and large surface areas.

According with the literature,  $\text{Li}_2\text{SiO}_3$  practically does not react with  $\text{CO}_2$  in this temperature range under dry conditions, due to kinetic factors. Nevertheless, the results presented here showed that water addition improves the  $\text{CO}_2$  capture on this ceramic. From this point of view, these results suggest that water vapor addition may improve the  $\text{CO}_2$  capture on other lithium ceramics.

#### Acknowledgments

This work was financially supported by the ICyT-DF (179/2009) and PAPIIT-UNAM (IN100609) projects. J. Ortiz-Landeros thanks to CONACYT and PIFI-IPN for financial support. Authors thank to Miguel A. Canseco for technical help.

#### References

- [1] N. Roux, S. Tanaka, C. Johnson, R. Verrall, *Fus. Eng. Des.* 41 (1998) 31.
- [2] D. Cruz, S. Bulbulian, *J. Nucl. Mater.* 312 (2003) 262.
- [3] R. Knitter, B. Alm, G. Roth, *J. Nucl. Mater.* 367–370 (2007) 1387.
- [4] H. Pfeiffer, P. Bosch, S. Bulbulian, *J. Nucl. Mater.* 257 (1998) 309.

- [5] Y. Tomita, H. Matsushita, H. Yonekura, Y. Yamauchi, K. Yamada, K. Kobayashi, *Solid State Ionics* 174 (2004) 35.
- [6] Y. Abe, E. Matsui, M. Senna, *J. Phys. Chem. Solids* 68 (2007) 681.
- [7] D.R. Zhang, H.L. Liu, R.H. Jin, N.Z. Zhang, Y.X. Liu, Y.S. Kang, *J. Ind. Eng. Chem.* 13 (2007) 92.
- [8] J.W. Fergus, *Sensors Actuators B* 134 (2008) 1034.
- [9] N. Imanaka, Y. Hirota, G.Y. Adachi, *Sensors Actuators B* 425 (1995) 380.
- [10] R. Xiong, I. Ida, Y.S. Lin, *Chem. Eng. Sci.* 58 (2003) 4377.
- [11] B.N. Nair, R.P. Burwood, B.J. Goh, K. Nakagawa, T. Yamaguchi, *Prog. Mater. Sci.* 54 (2009) 511.
- [12] J.D. Figueroa, T. Fout, S. Plasynski, H. Mcllvried, R.D. Srivastava *Inter., J. Greenhouse Gas Control* 2 (2008) 9.
- [13] ACS Symposium Series (1056), *Advances in CO<sub>2</sub> conversion and utilization*, in: Yun Hang Hu, (Ed.), *Advances on Alkaline Ceramics as Possible CO<sub>2</sub> Captors*, Chapter 15, H. Pfeiffer, Washington DC, USA, 2010, pp. 233–253, ISBN: 978-0-8412-2596-1.
- [14] D. Cruz, S. Bulbulian, E. Lima, H. Pfeiffer, *J. Solid State Chem.* 179 (2006) 909.
- [15] T. Tang, Z. Zhang, J.B. Meng, D.L. Luo, *Fus. Eng. Des.* 84 (2009) 2124.
- [16] S.I. Furusawa, A. Kamiyama, T. Tsurui, *Solid State Ionics* 179 (2008) 536.
- [17] S.I. Furusawa, T. Kasahara, A. Kamiyama, *Solid State Ionics* 180 (2009) 649.
- [18] Y.P. Naik, M. Mohapatra, N.D. Dahale, T.K. Seshagiri, V. Natarajan, S.V. Godbole, *J. Lumin.* 129 (2009) 1225.
- [19] S. Morimoto, S. Khonthon, Y. Ohishi, *J. Non-Cryst. Solids* 354 (2008) 3343.
- [20] B. Zhang, M. Nieuwoudt, A.J. Easteal, *J. Amer. Ceram. Soc.* 91 (2008) 1927.
- [21] R.B. Khomane, B.K. Sharma, S. Saha, B.D. Kulkarni, *Chem. Eng. Sci.* 61 (2006) 3414.
- [22] G. Mondragón-Gutiérrez, D. Cruz, H. Pfeiffer, S. Bulbulian, *Res. Lett. Mater. Sci.* 2 (2008) 1.
- [23] J. Ortiz-Landeros, M.E. Contreras-García, C. Gómez-Yáñez, H. Pfeiffer, *J. Solid State Chem.* 184 (2011) 1304.
- [24] K.S.W. Sing, D.H. Everett, R.A.W. Haul, L. Moscou, R.A. Pierotti, J. Rouquerol, T. Siemieniewska, *Pure Appl. Chem.* 57 (1985) 603.
- [25] K. Sing, *Coll. Surf. A: Physicochem. Eng. Asp.* 187–188 (2001) 3.
- [26] G. Leofanti, M. Padovan, G. Tozzola, B. Venturelli, *Catal. Today* 41 (1998) 207.
- [27] FACTSage Thermochemical Software and Databases <www.factsage.com>.
- [28] E. Ochoa-Fernandez, T. Zhao, M. Ronning, D. Chen, *J. Environ. Eng.* 135 (2009) 397.
- [29] K. Essaki, K. Nakagawa, M. Kato, *J. Chem. Eng. Jpn.* 37 (2004) 772.
- [30] R. Siauciunas, E. Rupsyte, S. Kitrys, V. Galeckas, *Coll. Surf. A. Physicochem. Eng. Asp.* 224 (2004) 197.
- [31] L. Martínez-dlCruz, H. Pfeiffer, *J. Phys. Chem. C* 114 (2010) 9453.
- [32] V.C. Farmer, *The Infrared Spectra of Minerals*, Mineralogical Soc. Monographs, Mineral. Soc. Press, (1977).
- [33] K. Nyquist, *Infrared Spectra of Inorganic Compounds*, Academic Press, Inc., United Kingdom, 1971.
- [34] H. Pfeiffer, E. Lima, V. Lara, J.S. Valente, *Lang.* 26 (2010) 4074.
- [35] J. Ortiz-Landeros, L. Martínez-dlCruz, C. Gómez-Yáñez, H. Pfeiffer, *Thermochim. Acta* 515 (2011) 73.